Multi-Range Approach of Stereo Vision for Mobile Robot Navigation in Uncertain Environments

Kwang Ho Park*

Automation and Componenrs Divsion, Korean Agency for Teclutology and Standards,
#2 Jungang-dong, Gwacheon, Gyeonggi-do 427-716, Korea

Hyung O Kim

SamSung Electronics co., LTD.
416, Maetan-dong, Paldal-gu, Suwon, Gyeonggi-do 442-742, Korea

Moon Yeol Baek

Department of Automobile & Machinery, SunCheon First College
9-3, Deokwal-dong, Suncheon, Chonnam 540-744, Korea

Chang-Doo Kee

Department of Mechanical Engineering, Chonnam National University,
300, Yongbong-dong, Buk-gu, Gwangju 500-757, Korea

The detection of free spaces between obstacles in a scene is a prerequisite for navigation of a mobile robot. Especially for stereo vision-based navigation, the problem of correspondence between two images is well known to be of crucial importance. This paper describes multi-range approach of area-based stereo matching for grid mapping and visual navigation in uncertain environment. Camera calibration parameters are optimized by evolutionary algorithm for successful stereo matching. To obtain reliable disparity information from both images, stereo images are to be decomposed into three pairs of images with different resolution based on measurement of disparities. The advantage of multi-range approach is that we can get more reliable disparity in each defined range because disparities from high resolution image are used for farther object a while disparities from low resolution images are used for close objects. The reliable disparity map is combined through post-processing for rejecting incorrect disparity information from each disparity map. The real distance from a disparity image is converted into an occupancy grid representation of a mobile robot. We have investigated the possibility of multi-range approach for the detection of obstacles and visual mapping through various experiments.

Key Words : Stereo Matching, Camera Calibration, Occupancy Grid Map, Mobile Robot

1. Introduction

Detection of obstacles and free spaces in scene is an essential function of vision-based mobile robot. Even if a map of the environment is given, this function is indispensable for coping with unknown obstacles in the map. Many researchers have been working on geometric modeling of the environment from sensory data. Most of them use a laser range finder or an ultrasonic sensor when object identification is not needed or only navigation is considered. Visual information is often used for feature tracking (Hager, 1994) or landmark sensing (Betke et al., 1997). Especially, stereo vision approaches are highly desirable for

---

* Corresponding Author,
  E-mail : pkh0920@ats.go.kr
  TEL : +82-2-509-7353; **FAX** : +82-2-509-7324
  Automation and Componenrs Divsion, Korean Agency for Teclutology and Standards, #2 Jungang-dong, Gwacheon, Gyeonggi-do 427-716, Korea. (Manuscript Received May 22, 2002; **Revised** July 9, 2003)

object recognition and also are important in many situations where active ranging methods are not feasible.

The two key problems of stereo vision system for a mobile robot have to be considered. One is how to correct camera calibration for removing lens distortion. Camera calibration is important for an accurate representative of the real world. This distortion caused by lenses displaces points in the image plane inwards or towards from its optical center (Tsai, 1987 ; Heikkila et al., 1997). The distortion effect of camera with high quality is negligible but its effect for low cost lens with wide field of view is and significant has to be taken into account. This distortion significantly can change positions of points in the image of a scene acquired by a camera. It affects both of the correct determination of point correspondences and the computation of disparities between points. Furthermore, this error increases when range values are extracted from disparities of stereo image. The other is how to find the correspondence points in the left and right image fast and efficiently. A large number of methods have been developed to solve the stereo matching problem. The existing techniques for stereo matching are grouped into two categories according to the matching primitives :

- Feature-based approach
- Area-based approach

The feature-based approaches (Pilu, 1997) extract image features such as edges, lines and corners for matching them across stereo images. These methods can produce fast and robust matching but depend on feature extraction to locate reliable features in the two images and yield only sparse depth maps. The area-based approaches (Kanade et al., 1994 ; Jennings et al., 1999) compare small area patches among both images using correlation and produce dense depth maps. The special issue in vision-based navigation is the design of relatively stable and fast matching algorithm for the stereo reconstruction. The choice of stereo approaches always depends on the objective of the application. For a successful reconstruction of complex surfaces, it is essential to

compute dense disparity maps for every pixel in the entire image. Since most stereo systems provide sparse range data, it is necessary to determine object regions. Unfortunately, most of the existing dense stereo techniques are very difficult in practical applications. This paper describes multi-range approach for area-based stereo matching and grid mapping of a mobile robot in uncertain environments. Camera calibration parameters are optimized by evolutionary algorithm for successful stereo matching. To obtain reliable disparity information from both images, stereo images are to be decomposed into three pairs of images with different horizontal resolution based on measurement of disparities. The reliable disparity map is composed of a combination of correct disparity information from each image. The real distance from a disparity image is converted into an occupancy grid representation for vision-based navigation of a mobile robot. Experimental results show that these approaches are a possible solution for vision-based navigation. In the next section, we introduce the camera calibration using evolutionary algorithm for depth reconstruction. Section 3 describes the basic idea of the proposed stereo matching method. In section 4, we show the examples of experimental results and finally conclude the paper.

2. Camera Calibration

2.1 Camera calibration

The main task of camera calibration in vision is to obtain an optimal set of the intrinsic and extrinsic camera parameters using known control points in the image and their corresponding 3D points in the world coordinate system. By using the pinhole model, the projection of the point $^cP_i = [^cX_i \ ^cY_i \ ^cZ_i]^T$ to the image plane as shown in Fig. 1 is expressed as

$$\begin{bmatrix} x_i \\ y_i \end{bmatrix} = \frac{f}{^cZ_i} \begin{bmatrix} ^cX_i \\ ^cY_i \end{bmatrix} \qquad (1)$$

The corresponding image coordinates $[u_i \ v_i]^T$ in pixels are obtained from the projection $[x_i \ y_i]^T$ by applying the following transformation
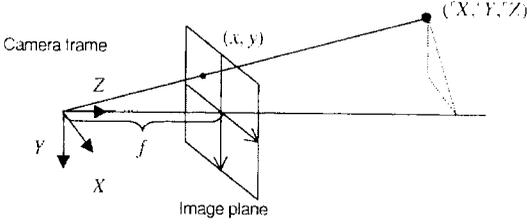
Fig. 1 Camera model

$$\begin{bmatrix} u_i \\ v_i \end{bmatrix} = \begin{bmatrix} a_x x_i \\ a_y y_i \end{bmatrix} + \begin{bmatrix} u_o \\ v_o \end{bmatrix} \qquad (2)$$

where a_x and a_y are the number of image points in horizontal and vertical dimensions, respectively. The intrinsic camera parameters usually include the effective focal length f and the principal point (u_o, v_o). Usually, the pinhole model is extended with some corrections for the systematically distorted image coordinates. The most commonly used correction is for the radial lens distortion. Therefore, camera calibration model can be written in the following form

$$\begin{bmatrix} u_i \\ v_i \end{bmatrix} = \begin{bmatrix} a_x(x_i + x_i(k_1 r^2 + k_2 r^4)) \\ a_y(y_i + y_i(k_1 r^2 + k_2 r^4)) \end{bmatrix} + \begin{bmatrix} u_o \\ v_o \end{bmatrix} \quad (3)$$

where k_1, k_2 are coefficients for radial distortion and $r = \sqrt{x_i^2 + y_i^2}$.

2.2 Solving for camera parameter using genetic algorithm (GA)

The camera parameters can be usually solved using nonlinear estimation technique due to the distortion model. If a good initial guess of the conventional optimization algorithm is not chosen before starting nonlinear search, the solution can diverge or get trapped in a local minimum. We use genetic algorithms as alternative to conventional optimization for camera parameter estimation. GA is well known that it has a good performance in solving optimization problems since it employs parallel search (Se et al., 2001). In this paper, distortion factors are added to GA method proposed by Qiang Jui (2001) for camera calibration.

2.2.1 Representation

The system being evolved is encoded into a long bit string called a *chromosome*. Each feature of the system located at a specific position in the string is called a *gene*. Initially a large random set of strings, population, is generated. If **C** be a vector consisting of the unknown intrinsic and extrinsic parameters, **C** is expressed as

$$\mathbf{C} = [f, u_o, v_o, k_1, k_2, a, \beta, \gamma, X, Y, Z]^T \quad (4)$$

Each camera parameter **C** as the chromosome vector is initialized to a value within its respective lower and upper bounds.

$$\mathbf{C}_i^t = (C_1, C_2, \cdots, C_n) \qquad 1 \le i \le N \qquad (5)$$

where N and n denote the population size and the number of parameters, respectively, and t is a number of generation.

2.2.2 Evaluation

The optimal solution **C** with control points can be obtained by minimizing the distance in the image plane between the points and the projected reference points (U, V).

$$F_{object} = \sum_{i=1}^{m} [(U_i - u_i(\mathbf{C}, {}^c\mathbf{P}_i))^2 + (V_i - v_i(\mathbf{C}, {}^c\mathbf{P}_i))^2] \quad (6)$$

2.2.3 Crossover and mutation

The genetic process is based on two genetic operator, crossover and mutation, to produce a new population from the selected population. The crossover operator is a method for exchange a partial set of attributes between design pairs selected probabilistically from the population, based on a crossover probability p_c. Let $\mathbf{C}_i^t$ and $\mathbf{C}_{i+1}^t$ be two individuals from population N at generation t. New individuals in generation $t+1$ can be expressed as a linear combination of two arbitrarily selected individuals from the previous generation t.

$$\mathbf{C}_i^{t+1} = (1 - p_c) \mathbf{C}_i^t + p_c \mathbf{C}_{i+1}^t \qquad (7)$$

$$\mathbf{C}_{i+1}^{t+1} = (1 - p_c) \mathbf{C}_{i+1}^t + p_c \mathbf{C}_i^t \qquad (8)$$

A mutation operator arbitrarily alters one or more components of a selected structure so as to increase exploration of other areas in the design search space by the mutation probability. Here is used reciprocal mutation as mutation operator.

Table 1 Bounds of camera parameters

Parameter	Limits (unit)
f	[6, 9] (mm)
u_o, v_o	[220, 360] (pixel)
k_1, k_2	[−0.001, 0.001]
α, β, γ	[−$\pi/4, \pi/4$] (radian)
X, Y	[900, 500] (mm)
Z	[−2000, −1000] (mm)

Table 2 Parameters of genetic algorithm

GA parameter	Value
Population size	$N=100$
Probability of crossover	$p_c=0.8$
Probability of Mutation	$p_m=0.1$
Elitist method	Yes
Coding method	Real coding

Fig. 2 Calibration result

(a) Error in X direction (b) Error in Y direction

Fig. 3 Difference between the original and corrected points

2.3 Experimental results

We applied GA-based method to real images for camera calibration. Table 1 shows a reasonable lower and upper bounds of both camera parameters in experiments. GA parameters for experiments are shown in Table 2.

Figure 2 shows the comparison between real dot points (+) and corrected points (o), where the corrected data is generated using distortion coefficients k_1 and k_2 of calibration results. We can notice the severe distortion toward the ends of the raw image. The effects of distortion are seen as bowing of what to be straight lines and the raw image is corrected by camera calibration. The correction of lens distortion makes parallel lines of dots in test image. Figure 3 shows differences between the original and corrected points in horizontal and vertical directions. We can observe that the maximum difference is more than 5 pixels at the corners of images while there is no distortion in the center of images.

3. Multi-Range Approach for Stereo Matching

3.1 Area of interest

We define *area of interest* (AOI) in both images since we care about unknown obstacles on ground plane of corridor or hallway. it is reasonable to limit the processing region because the upper and bottom areas are too far or close to recognize and are less important than those in the *area of interest*. The purpose for definition of *area of interest* is to reduce processing time and to concentrate on the region of corridor and unknown objects into corridor.

3.2 Multi-range approach for estimation of disparity

Our idea behind the multi-range approach was inspired by the multi resolution method with a uniform search model of Luca Locchi (1998). However, our approach separates regions with different range a based on the measurements of disparities. We plotted the range or depth as a function of disparity for our camera by known stereo geometry, as shown in Fig. 4. The mini-

mum range in this plot is 500 mm with disparity of 48 pixels, whereas the maximum range is about 15 meters. However most of the meaningful range in disparity occurs at 5 meters approximately. If we set the allowable limits of range resolution 100 mm. We can trust large disparity data because the resolution at closer ranges is much better than at further ranges. However with large search region of disparities, it takes longer to detect close objects with reliable resolution.
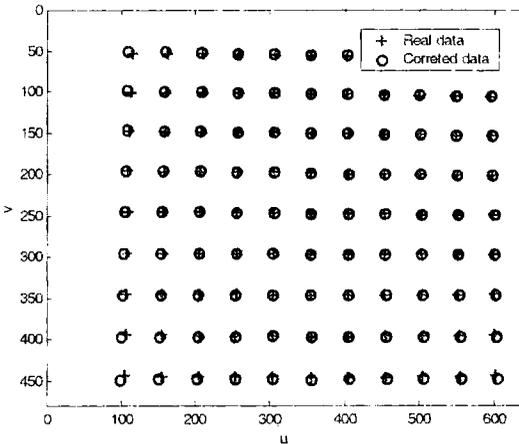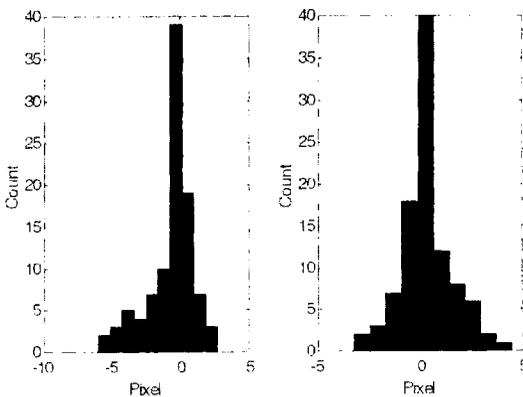
Therefore, we decomposed the range into three regions according to the measured disparity values in each Range defined, as shown in Fig. 4. For each range, we have three pairs of images with different horizontal resolution as follows.

• Range I : Low resolution image for detection of close object $(d_L^{min} < d_L < d_L^{max})$. In this range, large disparity has high confidence because close objects are needed in large search block. Small disparity can mismatch or cause errors.

• Range II : Medium resolution image $(d_M^{min} < d_M < d_M^{max})$

• Range III : High resolution image for detection of objects $(d_H^{min} < d_H < d_H^{max})$ further away. Contrary to Range I, small disparity has higher confidence than large disparity because of small search size and high resolution.

The advantage of multi-image scheme is that we can find more reliable disparity in each region because disparities from high resolution images are used for objects further away, while disparities from low resolution images are used for close objects. Another advantage is that the range for close objects can be obtained without increasing computational time by horizontal search size of disparity. The same stereo algorithm is applied
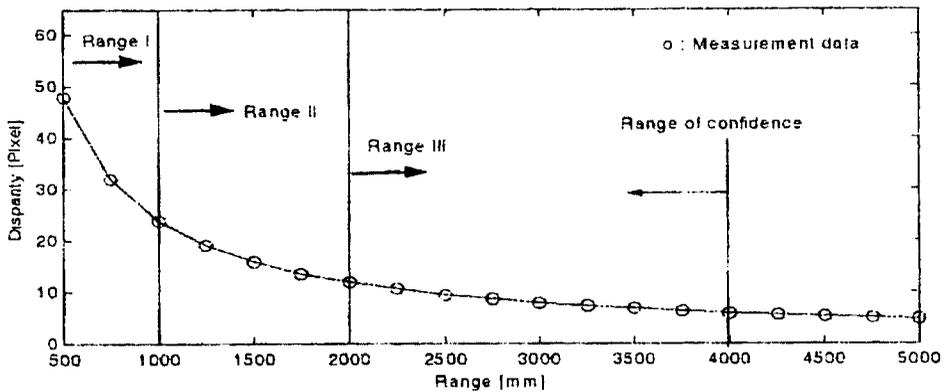
(a) Disparity and depth
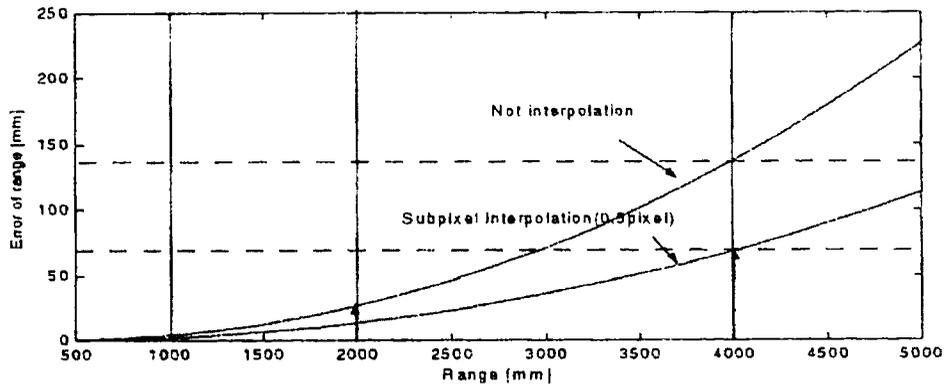
(b) Range resolution

Fig. 4 Experimental results of disparity mesurement
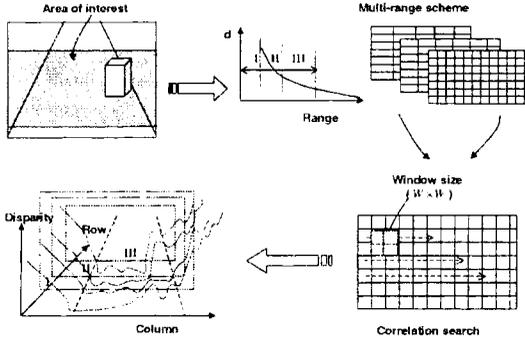
Fig. 5 Proposed stereo matching method

independently to images at different resolutions, and then combines the disparities by applying the rejection procedure for remove incorrect disparity. Figure 5 shows proposed multi-range stereo matching approach.

3.3 Area correlation matching

Area correlation-matching has been investigated extensively for many applications (Heikkila et al., 1997 ; Faugeras et al., 1993). Our work is based on block matching algorithm proposed by Andrea Fusiello (2000). As the matching measures, Normalized sum-of-squared differences (SSD) for grayscale images is defined as

$$SSD(x, y, d)$$
$$= \frac{\sum_{i=-w}^{u}\sum_{j=-w}^{w}[I_L(x+i, y+j)-I_R(x+i+d, y+j)]^2}{\sqrt{\sum_{i=-w}^{w}\sum_{j=-w}^{w}I_L(x+i, y+j)^2 \sum_{i=-w}^{w}\sum_{j=-w}^{w}I_R(x+i+d, y+j)^2}} \quad (9)$$

where $I_L(u, v)$ and $I_R(u, v)$ denote left image and right image respectively and d is disparity for search (min $d \le d \le$ max d). Area correlation compares small patches, window size ($W \times W$) among images using correlation. The measure of correlation is applied to all rows of interest area in left image. The disparity estimation for pixel is the one that minimize the SSD error.

$$d(x, y) = \arg\min_d SSD(x, y, d) \quad (10)$$

3.4 Combination of multi-disparity map

The stereo matching data usually contain errors due to noise and un-textured area. To reduce

these errors, median filter is applied before combining of the disparity results. Post-processing is used to reject incorrect disparity information from each disparity map before the maps are combined. Reliable disparity could be obtained through three steps following,

Step 1. Find the disparity range in the defined Range (k) $(k=1, 2, 3)$ in the multi-resolution images. If d_k is a disparity set of Range k, confident disparity is recomposed as follows :

$$d_k(x, y)$$
$$= \{ d \mid d_k(x, y) \in [Range(k)^-, Range(k)^+] \} \quad (11)$$

where $Range(k)^-$ and $Range(k)^+$ means the upper and lower bounds of each range, respectively, that are determined from the relationship between disparity and range.

Step 2. Build the same horizontal size through up-sampling procedure because low and medium image are smaller than the original image.

Step 3. Combine the confident disparity d_k of each range. This combination means that incorrect disparity is rejected or replaced with reliable data obtained from Step 1.

$$\hat{d}(x, y) = d_1(x, y) \oplus d_2(x, y) \oplus d_3(x, y) \quad (12)$$

where $\oplus$ means union of sets d_1, d_2 and d_3.

3.5 Rejection of disparity

Estimated disparity data usually contain poor quality data such as wrong matching or ghost points from uniform areas such as ground plane. Therefore, to suppress uncertain range data of ground plane with no texture in the image, these statistical variations of uniform ground plane can be modeled as Gaussian distribution with small standard deviation of gray patches in ground plane. In typical static image, we have measured means μ_{patch} and standard deviation σ_{patch} in the gray image with ground areas.

$$\hat{d}(x, y) = \begin{cases} 0 & \text{if } (\mu_{patch}, \sigma_{patch}) \le T \\ \hat{d}(x, y) & \text{otherwise} \end{cases} \quad (13)$$

where T is experimental threshold value for suppression of ground plane area.

The geometry of the stereo setting computes the 3D coordinates of feature points matched in the

images by following expression.

$$Z = \frac{b \cdot f}{\hat{d}} \qquad (14)$$

$$X = (x_i \cdot Z)/f \qquad (15)$$

$$Y = (y_i \cdot Z)/f \qquad (16)$$

where f is a focal length and b is a base line distance between two cameras.

4. Experiments

The visual mapping system described in this paper has been implemented on a mobile robot that we developed as shown in Fig. 6. It has RC caterpillar with two DC-motors driven by a PWM and a controller based on a micro-controller 80C196K. The total system is composed of a mobile robot, stereo cameras and PC-based vision systems. A stereo vision head with two CCD cameras provides a resolution of 320×240 pixels. The robot is also equipped with two RF communication modules that allow wireless
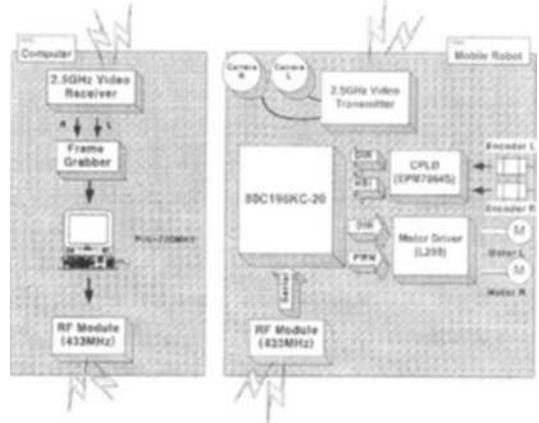
Fig. 6 Configuration of system hardware

(a) Left image

(b) Right image

(c) Combination of disparity map
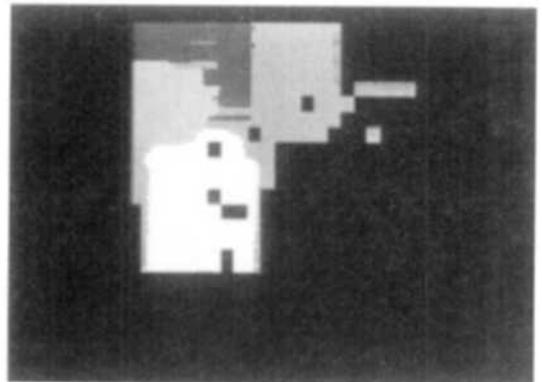
(d) Dense map after ground suppression

Fig. 7 Disparity map

communication to a host computer with frame grabber to send image data and receive control data.

Figure 7 shows test scene with three objects located in corridor. Fig. 7(c) and (d) show disparity results by proposed method and dense map after ground suppression. Figure 8(a) shows the details of multi-resolution image and the results of disparity map after implementation of the rejection procedure of dense disparity data of a low resolution image (Range I). The stereo results can be interpreted directly as range information. The top view of the depth-by-column projection of the modified disparity in Range I is shown in Fig. 8(b). We note that an unknown object that is the closest exists in the confident region of range I (500 mm ~ 1000 mm), and depth resolution is more robust than other Range areas.

Figures 9 and 10 show modified disparity maps

and the top view of depth after the implementation of the rejection procedure in medium and high resolution (Range II and III), respectively. The range results are very sensitive to disparity value. The sparse outline errors of second and third objects are due to mismatching data in the uniform area. However, depth error can be decreased or improved by forward movement of a robot. From the experimental results, we found that the robot could distinguish between the ground plane and objects at a distance of up to about 4 m at the same time. The range accuracy of objects is sensitive to errors in camera calibrations like lens distortion and camera rectification.

5.2 Experiments for grid mapping of corridor profile

We have investigated the possibility of stereo
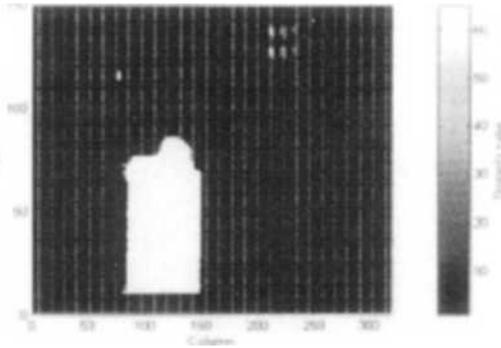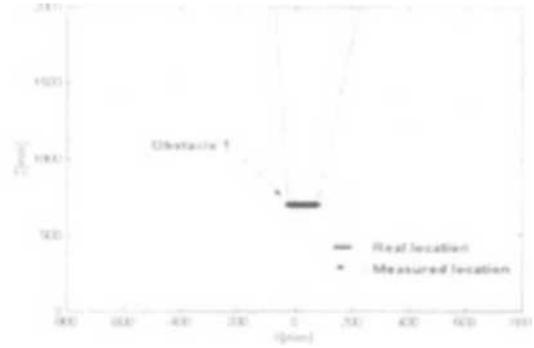
(a) Results of disparity map   (b) Top view of depth

Fig. 8 Disparity map of Range I
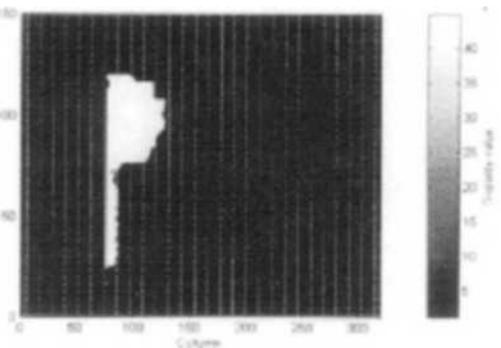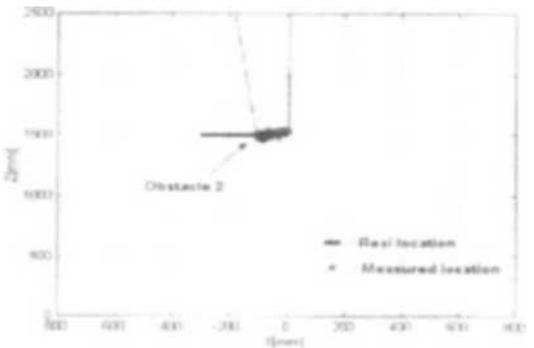
(a) Results of disparity map   (b) Top view of depth

Fig. 9 Disparity map of Range II

matching method for the visual mapping through various experiments. Occupancy map generation was tested at the corridor of our office building where there is no obstacle. The office building is mainly composed of straight lines and corners. The objective of these experiments was to see how well our vision system could represent the profile of the corridor, a type of uncertain environment. Cameras were calibrated and rectified to achieve successful stereo matching. Utilizing the stereo dense disparity, the robot built a map of the indoor environment as shown in Fig. 11. The corridor model of a 12 m × 6 m region was

internally represented as grid map for navigation. The proposed stereo algorithm and ground suppression were applied in corridor images obtained following the robot path. The profiles of corridor were generated using three images in the scenes : front image, left and right images.

The front image includes only the information of obstacles in front of a mobile robot. The matching results give very narrow areas according to search disparity. For more wide view of field, both side view in direction of 45° are used to generate the map of a corridor. Figures 12 and 13 show the generation of distance map from both

(a) Results of disparity map   (b) Top view of depth
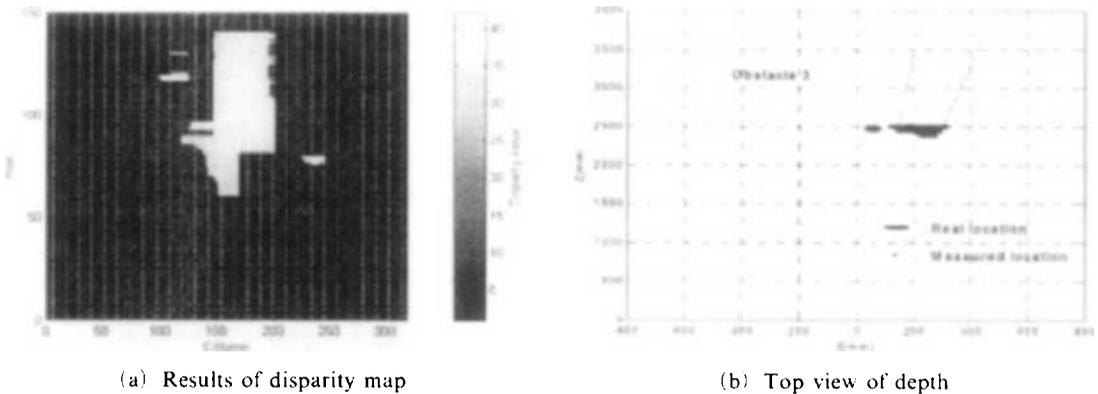
Fig. 10   Disparity map of Range III
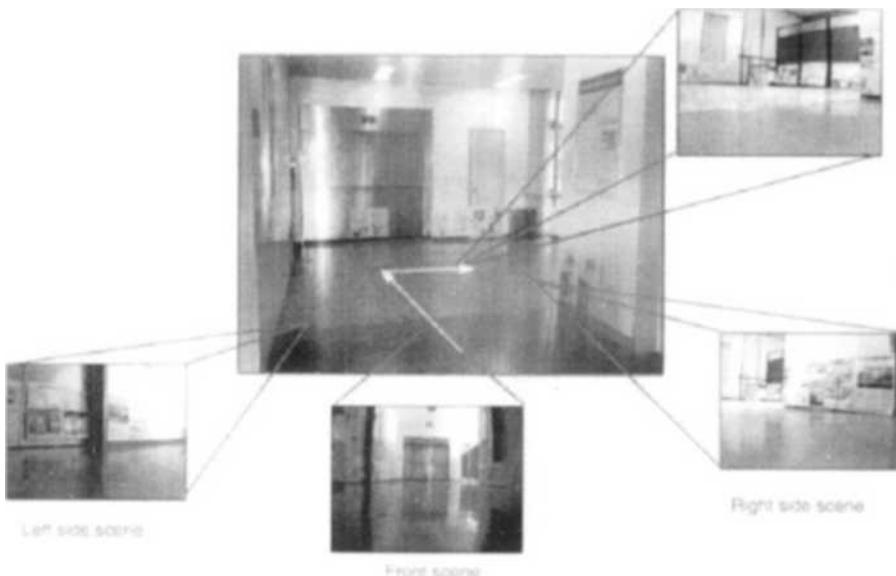
Fig. 11   Test corridor for stereo vision mapping
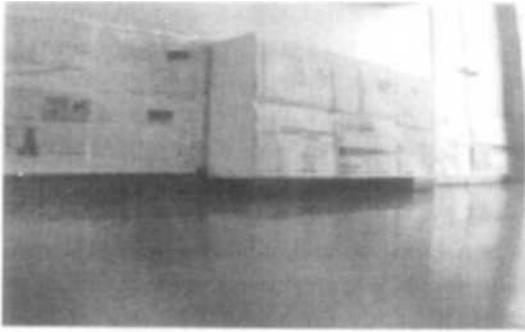
(a) Left wall image and disparity
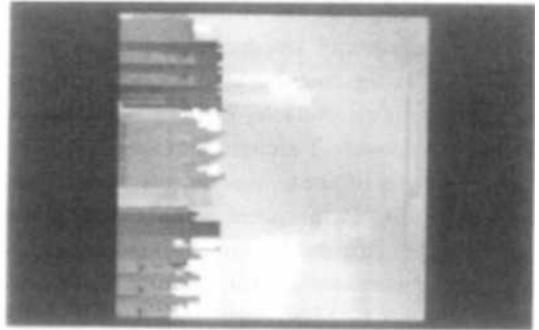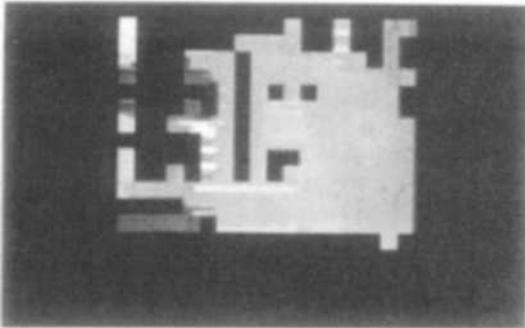
(b) Full disparity

(c) Texture rejection
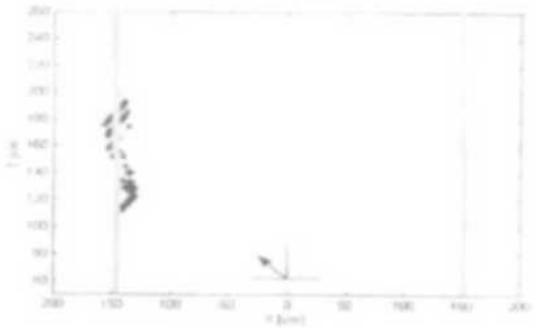
(d) Distance map

Fig. 12 Test corridor for stereo vision mapping (Left side view)
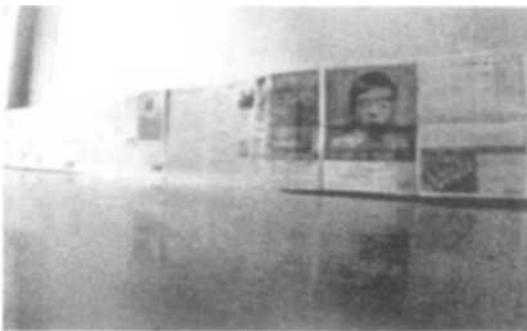
(a) Left wall image and disparity
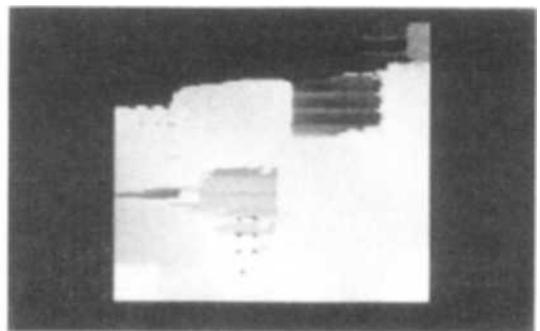
(b) Full disparity
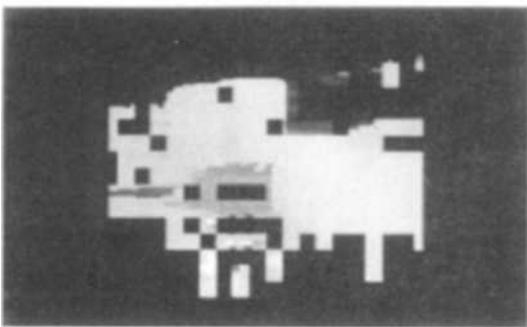
(c) Texture rejection
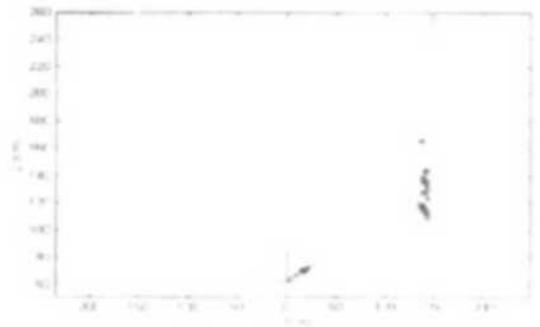
(d) Distance map

Fig. 13 Test corridor for stereo vision mapping (Right side view)
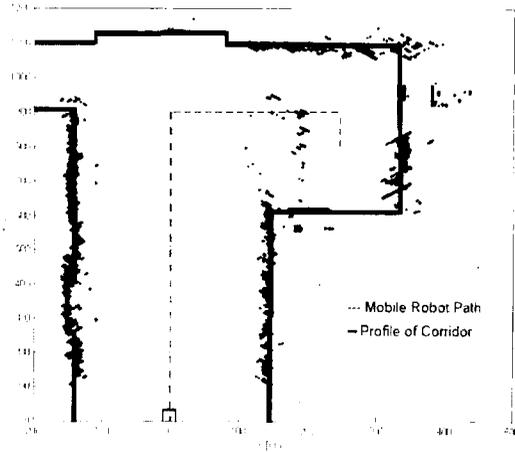
Fig. 14 Map generation using stereo-vision

side images, respectively. Figure 14 demonstrates the generated reliable results during a navigation experiment in corridor of office building. The occupied areas are indicated by dark gray dots and sold lines show top view of a real corridor. Some hallway areas have a slight bending effect of profile in straight hallway, which results from cumulative drift in the angle data of stereo head used to compute the robot's pose. Howerer, we notice that the profile of a hallway is clearly resolved in these maps. The sparse errors from ground of hallway can be observed from the map results. These errors are due to mismatching data that happen to over-illuminated ground plane or fluctuation of light source.

5. Conclusions

The detection of free spaces between obstacles in a scene is a prerequisite for navigation of a mobile robot and the problem of correspondence across two images is well known to be of crucial importance for vision-based mapping. This paper describes multi-range approach for area-based stereo matching and grid mapping for a mobile robot in an uncertain environment. Camera calibration parameters are optimized by evolutionary algorithm for successful stereo matching. To obtain reliable disparity information from both images, stereo images are to be decomposed into three pairs of images with different resolution based

on measurement of disparities. Stereo matching algorithm is applied and reliable disparity map is combined through post-processing for rejecting incorrect disparity information from each disparity map. The real distance from a disparity image is converted into an occupancy grid representation for vision-based navigation of a mobile robot. We have investigated the possibility of multi-range method for the visual mapping through experiments. Experiments show robust matching results between views, and results the present also show that the map built by combination of multi-disparity for occupancy is a possible solution for the mapping problem for a mobile robot.

References

Betke, M. and Gurvits, L., 1997, "Mobile Robot Localization Using Landmarks." *IEEE Transactions on Robotics and Automation*, Vol. 13(2), pp. 251~263.

Elfes, A., 1989, "Using Occupancy Grids for Mobile Robot Perception and Navigation," *Computer*, Vol. 22(6), pp. 46~57.

Faugeras, O. et al., 1993, "Real Time Correlation Based Stereo : Algorithm, Implementation and Applications," Research Report 2013, INRIA Sophia-Antipolis.

Faugeras, O., 1993, Three-Dimensional Computer Vision, MIT Press.

Fusiello, A. and Roberto, V., 2000, "Sysmmetric Stereo with Multiple Windowing," *International Journal of PRAI*, Nov. 14(8), pp. 1053~1066.

Fusiello, A., Trucco, E. and Verri, A., 2000, "A Compact Algorithm for Rectification of Stereo Pairs," *Machine Vision*, Nov. 12(1), pp. 16~22.

Hager, G. D., 1994, "Real-Time Feature Tracking and Projective Invariance as a Basis for Hand-Eye Coordination," *Proc. Computer Vision and Pattern Recognition*, pp. 533~539.

Heikkila, J. and Silven, O., 1997, "A Four Step Camera Calibration Procedure with Implicit Image Correction," *Int. IEEE Conference of Computer Vision and Pattern Recognition*. pp. 1422~1429.

Huber, M., MacDonald, W. S. and Grupen, R. A. 1996, "A Control Basis for Multi-Legged Walking," *IEEE Conference on Robotics and Automation*, Vol. 4, pp. 2988~2993.

Iocchi, L. and Konolige, K., 1998, "A Multi-resolution Stereo Vision System for Mobile Robots," *AIIA (Italian AI Association) Workshop*, pp. 124~131.

Jennings, C., Murry, D. and Little, J., 1999, "Cooperative Robot Localization with Vision based Mapping," *Proc. IEEE Conference on Robotics and Automation*, pp. 2659~2665.

Kanade, T. and Okutomi, M., 1994, "A Stereo Matching Algorithm with an Adaptive Window : Theory and Experiments," *IEEE Transactions on Patten Analysis and Machine Intelligence*, Vol. 16(9), pp. 920~932.

Kande, T., Yoshida, A., Oda, K., Kano, H. and Tanaka, M., 1996, "A Stereo Machine for Video-Rate Dense Depth Mapping and its New Application," *Proc. of Computer Vision and Pattern Recognition*.

Konolige, K., 1997, "Small Vision System : Hardware and Implementation," *8th International Symposium on Robotics Research*, pp. 2177~2182.

Moravec, H., 1996, "Robot Spatial Perception by Stereoscopic Vision and 3D Evidence Grids," *Carnegie Mellon University Technical Report* CMU-RI-TR-96-34.

Pilu, M., 1997, "A Direct Method for Stereo Correspondence based on Singular Value Decomposition," *Proc. Computer Vision and Pattern Recognition*, pp. 262~266.

Qiang Ji and Yongmian Zhang, 2001, "Camera Calibration with Genetic Algorithms," *IEEE Transaction on Systems, man and cybernetics part A : Systems and Humans*, Vol. 31, No. 2, pp. 120~130.

Se, S., Lowe, D. and Little, J., 2001, "Vision Based Robot Localization and Mapping using Scale Invariant Features," *Proc. IEEE Conference on Robotics and Automation*, Nov. 12~16, pp. 42~48.

Tsai, R. Y. 1987, "A Versatile Camera Calibration Technique for High Accuracy 3D Machine Vision Metrology Using off the Shelf TV Camera and Lenses," *IEEE Journal of Robotics and Automation*, Vol. 3(5), pp. 323~344.

Zhong, Y. and Ji, Q., 2001, "Camera Calibration with Genetic Algorithms," *IEEE Conference on Robotics and Automation*, pp. 2177~2182.